Application of fly ash-based geopolymer for removal of cesium, strontium and arsenate from aqueous solutions: kinetic, equilibrium and mechanism analysis

Quanzhi Tian and Keiko Sasaki

ABSTRACT

Geopolymerization is a developing reaction process for the utilization of solid wastes. In the present study, fly ash-based geopolymer and its derivative (Fe(II)-modified geopolymer) were synthesized and characterized using XRD, SEM, FTIR, BET, UV-Vis DRS as well as TG-DTA, and adopted as adsorbents for removal of Cs^+ and Sr^{2+}, and AsO_4^{3-} from solutions. Each sorption kinetic was well fitted to the pseudo-second-order model. The sorption of Cs^+ and Sr^{2+} onto original geopolymer were better fitted to the Langmuir model. However, the Freundlich model is more befitting for sorption of AsO_4^{3-} onto Fe(II)-modified geopolymer. The free energies calculated from the D-R isotherm indicated that the sorption for Cs^+ and Sr^{2+} were dominantly ion exchanges. Ring size plays a decisive role in ion exchanges for both Cs^+ and Sr^{2+}. Furthermore, the arrangement of SiO_4 and AlO_4 tetrahedrons has significant impacts on the ion exchange of Sr^{2+}. XPS results indicated that a part of Fe^{2+} in Fe (II)-modified geopolymer had been oxidized to Fe^{3+} after sorption. Precipitation of $FeAsO_4$ could partially contribute to the arsenate removal from solution. AsO_4^{3-}sorption has also occurred through the formation of inner-sphere complexes via ion exchange reaction, which could be predominantly attached by bidentate linkages.

Key words | coal fly ash, geopolymer, modification, sorption

Quanzhi Tian (corresponding author)
Keiko Sasaki
Department of Earth Resources Engineering,
Faculty of Engineering,
Kyushu University,
744 Motooka, Nishiku, Fukuoka 819-0395,
Japan
E-mail: *tianqz0502@foxmail.com*

INTRODUCTION

Geopolymers are a class of amorphous aluminosilicates with a three-dimensional structure consisting of SiO_4 and AlO_4 tetrahedrons, usually synthesized by low-temperature polycondensation of different materials such as metakaolin, and coal fly ash (Rożek *et al.* 2018). They always exhibit high compressive strength, high-temperature resistance, and permeability resistance, which provides tremendous potential to be a desirable alternative to ordinary Portland cement (Cho *et al.* 2017). Generally, the cations, such as Na^+ and K^+, would be located in the cavities of the framework in order to balance the negative charge produced by the AlO_4 tetrahedron. These charge-balancing cations can be exchanged with other cations, suggesting that geopolymer can be used as an adsorbent like zeolite in the removal of heavy metals from aqueous solutions. Water pollution by heavy metals is always a serious problem, which has been in the limelight for so many years (Uddin 2017). Currently, there are many approaches referring to heavy metal wastewater treatment, including adsorption, chemical precipitation, membrane filtration, ion exchange, and electrochemical treatment. Among them, adsorption, presenting the advantages of high efficiency, low cost, and a simple operation process, has been considered to be one of the most attractive options. The removal of Cu^{2+}, Pb^{2+}, Zn^{2+}, Mn^{2+}, Co^{2+}, Ni^{2+}, Cs^+, etc. by adsorption onto geopolymer has been conducted, resulting in good performances (El-Eswed 2018). However, geopolymer has a low affinity with anions, such as AsO_4^{3-}, SeO_4^{2-} (Al-Mashqbeh *et al.* 2018), because of the permanent negative charge on the AlO_4 tetrahedron. A chemical modification would be needed to apply geopolymer for anion removal. It has been shown that SO_4^{2-} can be effectively removed by barium-modified blast-furnace-slag geopolymer (Runtti *et al.* 2016).

Coal fly ash is an industrial waste composed of the fine particles that are captured from flue gases by electrostatic precipitators or other particle filtration equipment. Every year, large amounts of fly ash are generated over the world, which has been a serious environmental problem

doi: 10.2166/wst.2019.209

(Tian *et al.* 2019). Hence, synthesis of geopolymer could be a good way to consume coal fly ash and, meanwhile, the geopolymer could be used for other applications, which has great significance for the environment and economy. In order to evaluate the ability of fly ash-based geopolymer in adsorption of heavy metals, Cs^{+}, Sr^{2+} and AsO_4^{3-} were selected in this study. Cs^{+} and Sr^{2+} generally appear as radionuclides in nuclear waste effluents, so stabilization of them is required. Since they possess positive charges, it is appropriate to utilize geopolymer as an adsorbent directly. However, as discussed above, there is a low affinity between geopolymer and anion. Therefore, Fe(II)-modified geopolymer was developed for the removal of AsO_4^{3-} in this research. The detailed reaction mechanisms for these sorption processes are discussed and proposed.

EXPERIMENTAL

Materials

The coal fly ash used in this study was collected from a thermal power plant in China. The X-ray diffraction (XRD) pattern (Figure 1) shows that mullite and quartz are the main crystal minerals in the sample. The chemical composition of fly ash was determined using X-ray fluorescence spectroscopy (XRF, Rigaku ZSX Primus II). The result showed that the SiO_2 and Al_2O_3 contents in fly ash were 44.60 and 46.10%, respectively. The synthesis procedure of the geopolymer was as follows: the module of sodium silicate (SiO_2/Na_2O) was adjusted to 1.2 by adding sodium hydroxide. Then the activated solution was mixed with fly ash at a mass ratio of 0.67. After stirring for 10 min, the slurry was put into a mold with a diameter of 30 mm and thereafter treated by ultrasonication for 5 min in order to remove bubbles. The specimen was sealed with a plastic bag and cured at 80 °C for 12 h. Then it was cured at room temperature for another 18 h. The paste was then crushed and ground, then sieved to collect under 150 mesh sieve. Washing was conducted to remove the extra alkali. Lastly, the powder was dried at 105 °C overnight.

In addition, Fe(II)-modified geopolymer was prepared as followed: 5 g of geopolymer was put in 1 L of 0.1 mol·L^{-1} $FeSO_4$ with stirring under N_2 protection. After 20 h, the obtained solid was washed several times with deionized water that had dissolved O_2 removed through N_2 bubbling.

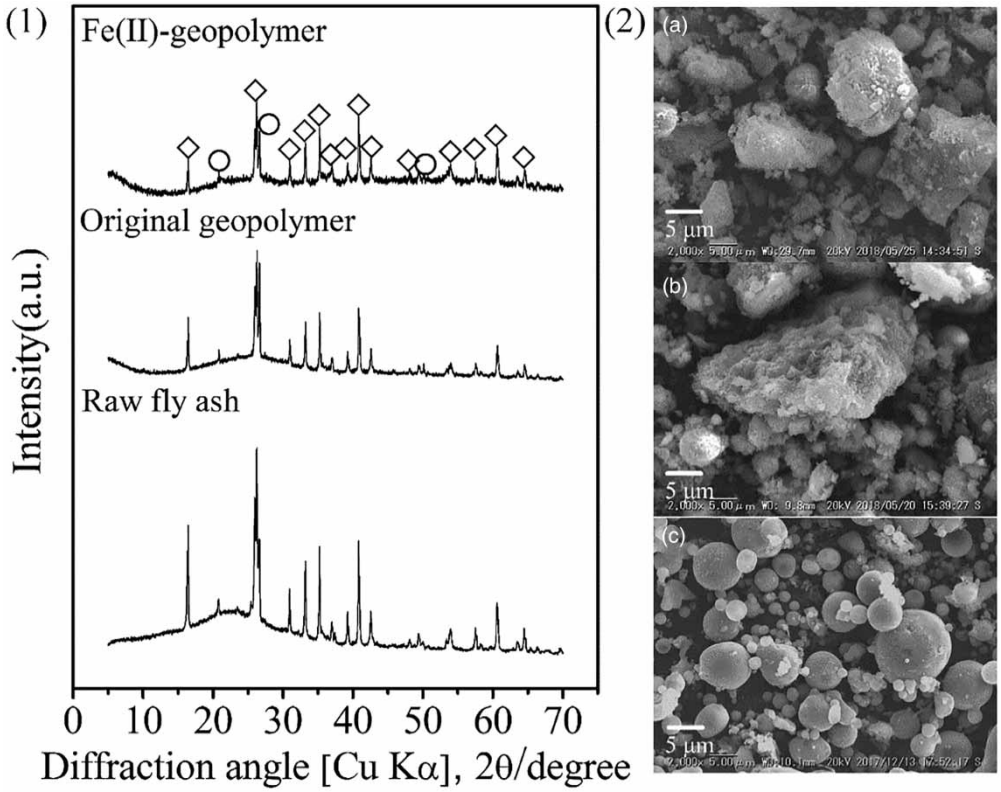

Figure 1 | (1) XRD patterns of raw fly ash, geopolymer and Fe(II)-modified geopolymer. Symbols: ◇, mullite ($3Al_2O_3{\cdot}2SiO_2$); ○, quartz (SiO_2); (2) SEM images of (a) coal fly ash, (b) geopolymer and (c) Fe(II)-modified geopolymer.

Then it was dried on a freeze dryer for 24 h and stored under N_2 protection. In addition, simulated pollutants Cs^+, Sr^{2+} and AsO_4^{3-} were prepared by dissolving proper amounts of CsCl (special grade, Wako), $SrCl_2{\cdot}6H_2O$ (special grade, Wako) and KH_2AsO_4 (90%, Wako) in deionized water, respectively.

Sorption experiments

50 mg of geopolymer or Fe(II)-modified geopolymer was taken and put in the 50 mL metal ion solution in variable concentrations at room temperature. Effects of solution pH and the concentration of adsorbent on the removal efficiencies were explored and the results are shown in Figures S1 and S2 (available with the online version of this paper). Thus, based on these results, experimental conditions were definite for kinetic and isotherm studies. The initial pH was adjusted to 7 for adsorbing Cs^+ and Sr^{2+}, and 5 for sorbing AsO_4^{3-}, respectively, by adding 0.1 mol·L^{-1} HCl or NaOH. Then the solutions were put on a magnetic stirrer for 24 h in order to reach equilibrium. Lastly, the 0.2 μm filter was used to remove fine particles from the solution for subsequent concentration determination. The amount of sorbed ions (q_e) was calculated by the equation below.

$$q_e = V(C_e - C_0)/m \quad (1)$$

where C_e and C_0 are the equilibrium and initial concentrations of metal ions (mmol·L^{-1}), V is the volume (L) and m is the weight of the adsorbent (g).

Kinetic studies were performed using the initial concentration of 100 mg/L in the case of Cs^+ and Sr^{2+} sorption onto the original geopolymer. For the AsO_4^{3-}, the initial concentration was 50 mg/L. For these investigations, 100 mg of adsorbent was added to beakers containing 100 mL solution with target pollutants. Then, the mixture was stirred using a magnetic stirrer at room temperature with an initial pH of 7 for Cs^+ and Sr^{2+}, and 5 for AsO_4^{3-}. Set volumes (1 mL) of aliquot were collected as a function of the contact time, while the solution was continuously stirred. The adsorbent in the collected solution was removed using a 0.2 μm filter.

Characterizations

The concentrations of Sr and As were determined using inductively coupled plasma optical emission spectrometry (ICP-OES, Perkin Elmer, Optima 8300, USA) and Cs was measured using inductively coupled plasma mass spectrometry (ICP-MS, Agilent 7500ce, USA). The XRD patterns were obtained at room temperature on a Rigaku Ultima IV XRD (Akishima, Japan): Cu Kα (40 kV, 40 mA) with a Ni filter at a scanning speed of 2° min^{-1} and scanning step of 0.02°. The Fourier transform infrared (FTIR) spectra (400–4,000 cm^{-1}) were recorded using an FTIR spectrometer (JASCO 670 Plus, Japan) with a resolution of 4 cm^{-1} employing powder samples diluted using KBr. The specific surface areas of raw fly ash and adsorbents were determined by a high-precision surface area and pore size distribution analyzer (BEL-Max, BEL, Japan) at −196 °C. Pre-treatment under vacuum at 100 °C for 15 h was conducted in order to remove adsorbed gas and water. In addition, thermogravimetric-differential thermal analysis (TG-DTA, 2000 SA thermal balance, Bruker, Germany) was used to determine the thermal properties of the adsorbent using α-Al_2O_3 as the reference material. The heating rate and nitrogen flow were 10 °C/min and 120 mL/min, respectively. Diffuse reflectance spectroscopy (DRS) was carried out in the range of 200–800 nm on a UV-2450 spectrophotometer equipped with a diffuse-reflectance attachment, using $BaSO_4$ as a reference. The dehydrated sample was prepared by calcining the original sample at 300 °C for 0.5 h with a heating rate of 10 °C/min and nitrogen flow of 120 mL/min. Scanning electron microscopy-energy dispersive X-ray spectroscopy (SEM-EDX) results were obtained from a VE-9800 SEM (Keyence, Osaka, Japan) with 20 kV acceleration voltages. X-ray photoelectron spectroscopy (XPS) was used to determine the chemical state of Fe in Fe(II)-modified geopolymer before and after adsorption of AsO_4^{3-}, performed on an ESCA 5800 (ULVAC-PHI, Inc., Kanagawa, Japan) using a monochromated Al Kα X-ray source. Here, the binding energy of C1s = 284.6 eV for adventitious carbon was adopted to calibrate the binding energies.

RESULTS AND DISCUSSION

Characterization of adsorbents

XRD patterns and SEM images of coal fly ash, original geopolymer and Fe(II)-modified geopolymer are shown in Figure 1. The main difference between them was the shift of the peak top of broad signals derived from the amorphous phase from approximately 23° for coal fly ash to almost 27° for geopolymer, indicating that the aluminosilicate glass phase in geopolymer was highly disordered. On the other hand, the XRD pattern of Fe(II)-modified geopolymer had no change compared to the original geopolymer. SEM images also indicated that the geopolymerization product

was formed with the comparison of the smooth spheres of raw fly ash. Even though a relative amount of fly ash still did not completely dissolve, the geopolymer had been formed and overlapped on the surface of fly ash particles. This is the pivotal point to use geopolymer and its derivative as adsorbents.

The infrared spectroscopic results for raw fly ash, geopolymer and Fe(II)-modified geopolymer are presented in Figure 2(a). There was a marked difference between the spectra of fly ash and geopolymer at around 3,463 and 1,657 cm^{-1} which were assigned to stretching and bending modes of the water molecule, respectively. In the spectrum of fly ash, there is no corresponding peak because fly ash does is not able to ion exchange, so the water molecule cannot be bound with metal ions as in geopolymer or its derivative. The intense peak at 1,114.2 cm^{-1} was attributed to the asymmetric stretching vibration mode of T–O–Si (T = Si or Al). For geopolymer, the band of T–O–Si were shifted to 1,058.2 cm^{-1}, which meant the rearrangement of SiO_4 and AlO_4 tetrahedrons. The peak at 580.6 cm^{-1} corresponded to the asymmetric stretching vibration of Si–O–Al and the band at 486.8 cm^{-1} was connected with the bending vibration O–Si–O in silicate tetrahedron. Blue shift and red shift occurred to these two bands, respectively. In addition, the stretching and bending vibrations of water molecules at 3,463.4 and 1,664.5 cm^{-1} in the spectrum of original geopolymer were shifted to 3,438.8 and 1,654.1 cm^{-1} for Fe(II)-geopolymer. This should be because Fe^{2+} has the larger polarizing power (charge/radius) and then stronger hydrogen bonds between the water molecules near Fe^{2+} would be formed (Madejová *et al.* 2002). Therefore, it can result in the bond length of O-H becoming longer, thereby leading to the wavenumber shifts of stretching vibration of them. In terms of other bonds including Si–O–Si, Si–O–Al, and O–Si–O, there were also some shifts that occurred to them. This was mainly because Fe^{2+} can be exchanged with Na^{+} in geopolymer, and this affected the local coordination chemistry.

Addition of the affinity with the anion to the geopolymer for anion can be an important modification in the stabilization/solidification of hazardous wastes. In the current study, the modification of geopolymer by Fe^{2+} was conducted and the obtained product presented a pale green color. The UV-Vis DRS spectra of original geopolymer and Fe(II)-geopolymer are shown in Figure 2(b). Compared to the original geopolymer, Fe(II)-geopolymer has a greater increase in adsorption in both the range of UV and visible

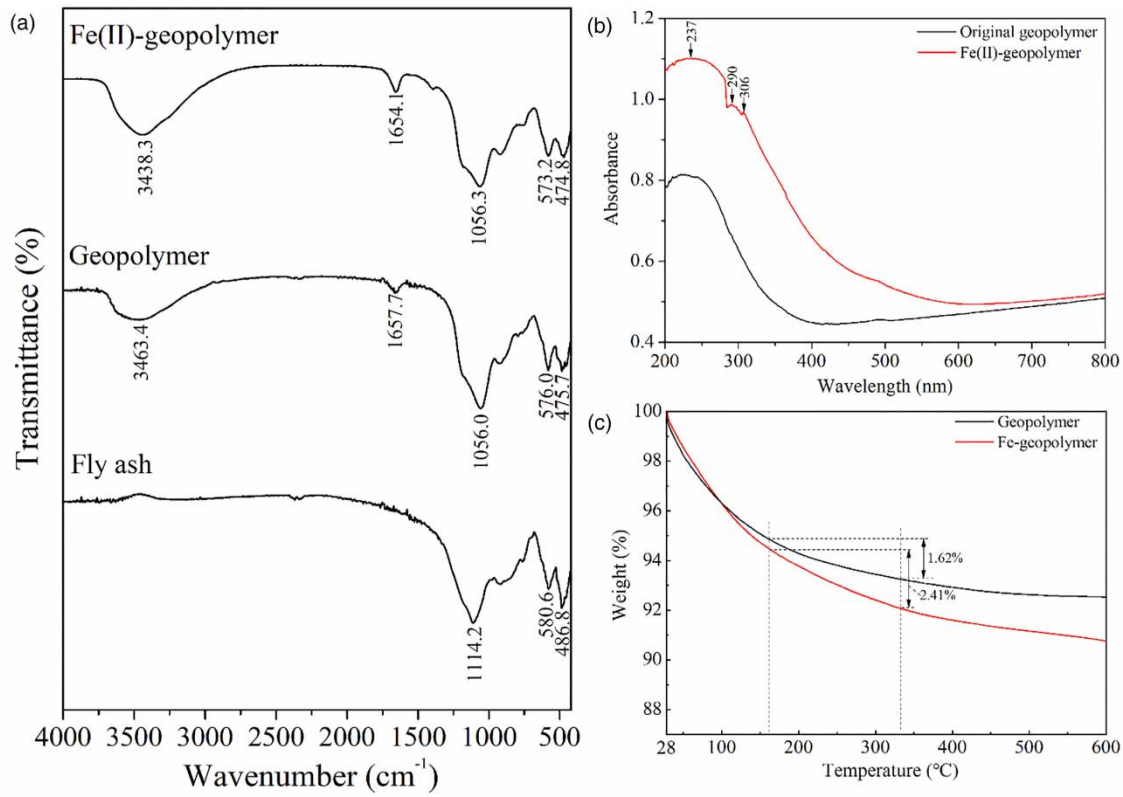

Figure 2 | (a) FTIR spectra of coal fly ash, geopolymer and Fe(II)-modified geopolymer; (b) UV-vis DRS spectra of dehydrated original geopolymer and Fe(II)-modified geopolymer; (c) TG-DTA curves of geopolymer and modified geopolymer.

light. Those bands at approximately 200–300 nm were assigned to the Fe-O charge-transfer transitions of Fe^{2+} in a tetrahedral and/or octahedral environment of oxygen atoms, which indicated that single Fe ions were present in cationic sites in the geopolymer.

TG curves of the original geopolymer and Fe(II)-modified geopolymer are presented in Figure 2(c). The weight loss at a temperature lower than 100 °C could be attributed to the loss of external weakly bound water molecules. The weight loss in the range of 160–330 °C is due to water molecules being more strongly bound to the mobile non-framework cations that are located in geopolymer cavities (Benaliouche *et al.* 2015). Greater weight loss happened in the case of Fe(II)-geopolymer (2.41%) than that of the original geopolymer (1.62%) at a temperature of 160–330 °C. It is obvious that cations with higher charge will interact more strongly with the unshared electron pair of the oxygen atom in the H_2O molecule. Hence, the formation of the hydrogen bond between one of the hydrogen atoms of the water molecule and the nearest framework oxygen will be favored when the cation with higher charge density acts as a charge balancing cation. On the other hand, Fe^{2+} has a smaller radius (0.076 nm) than that of Na^+ (0.095 nm), which indicates that there is more space for bound water in the cavities of geopolymer.

Nitrogen adsorption/desorption isotherms of raw fly ash, original geopolymer and Fe(II)-modified geopolymer are illustrated in Figure S4 (available with the online version of this paper). The specific surface area of raw fly ash was only 1.1 m^2/g according to the Brunauer–Emmett–Teller (BET) calculation of isotherm. However, the specific surface area of original geopolymer increased up to 131.4 m^2/g. As can be seen, a steep rise at low relative pressure ($P/P_0 < 0.01$) occurred in the adsorption curves of the original geopolymer, implying that micropore was produced after geopolymerization of coal fly ash. As for Fe(II)-geopolymer, the steep rise at low relative pressure ($P/P_0 < 0.01$) became lower compared to the original geopolymer, suggesting that the number of micropores decreased, thereby leading to the decrease of the specific surface area to 107.9 m^2/g. the influence on the surface area by multivalent cations is relatively complex. This behavior may be explained by the fact that the pores in geopolymer can be partially blocked by the cluster when Fe^{2+} is in large numbers at sites inside the cages (Lopes *et al.* 2015).

Sorption kinetics and isotherms

To describe the changes in the sorption of metal ions with time, the linearized forms of pseudo-first-order and pseudo-second-order kinetic equations are given as following Equations (2) and (3) (Lin & Wang 2009).

$$\text{Pseudo-first-order: } q_t = q_e(1 - e^{-k_1 t}) \quad (2)$$

$$\text{Pseudo-second-order: } q_t = \frac{k_2 q_e^2 t}{1 + k_2 q_e t} \quad (3)$$

where q_e and q_t (mmol/g) are the amounts of metal ions sorbed onto geopolymer or Fe(II)-geopolymer at equilibrium and at time t, respectively, and k_1 and k_2 are the rate constants (min^{-1}) of the pseudo-first-order and pseudo-second-order, respectively.

The fitting plots are shown in Figure S5 (available online), and the obtained parameters of each plot are summarized in Table 1. In case of the pseudo-second-order model, the correlation coefficient values for sorption of Cs^+ and Sr^{2+} onto the original geopolymer and the sorption of AsO_4^{3-} onto the Fe(II)-geopolymer were higher than the values for the pseudo-first-order. In addition, the calculated values of q_e for Cs^+ (0.346 mmol/g), Sr^{2+} (0.242 mmol/g) and AsO_4^{3-} (0.129 mmol/g) based on the pseudo-second-order model had good agreements with the experimental values of q_e for Cs^+ (0.351 mmol/g), Sr^{2+} (0.253 mmol/g) and AsO_4^{3-} (0.110 mmol/g). Therefore, it can be reasonably concluded that the adsorption kinetics of the systems including sorption of Cs^+ and Sr^{2+} onto original geopolymer and the sorption of AsO_4^{3-} onto Fe(II)-geopolymer fitted better with the pseudo-second-order model. This indicates that the overall rate constant of each sorption process appeared to be controlled by the chemical sorption.

In this study, isotherm models including Langmuir, Freundlich, and Dubinin-Radushkevich (D-R) were used to fit the equilibrium data for the sorption of Cs^+ and Sr^{2+} onto geopolymer and the sorption of AsO_4^{3-} onto Fe(II)-geopolymer. The linearized forms of Langmuir and

Table 1 | Calculated parameters of the pseudo-first-order and pseudo-second-order kinetic models for the sorption of Cs^+ and Sr^{2+} onto original geopolymer, AsO_4^{3-} onto Fe(II)-geopolymer

Kinetic model	Parameter	Cs^+	Sr^{2+}	AsO_4^{3-}
Pseudo-first-order	$q_{e,\,exp}$ (mmol/g)	0.351	0.253	0.110
	$q_{e,\,cal}$ (mmol/g)	0.338	0.234	0.108
	k_1 (min^{-1})	3.306	1.461	0.030
	R^2	0.985	0.954	0.967
Pseudo-second-order	$q_{e,\,cal}$ (mmol/g)	0.346	0.242	0.129
	k_2 (min^{-1})	23.173	12.509	0.266
	h (mmol g^{-1} min^{-1})	2.774	0.733	0.004
	R^2	0.998	0.977	0.983

Freundlich are written as Equations (4) and (5) (Ho 2006).

$$\text{Langmuir equation: } q_e = \frac{q_m b C_e}{1 + bC_e} \tag{4}$$

$$\text{Freundlich equation: } q_e = k_f c_e^{1/n} \tag{5}$$

where q_e is the amount of metal ion sorbed onto adsorbent (mmol/g), C_e is the equilibrium concentration of the metal ion in the equilibrium solution (mmol/L). Q_m is the monolayer adsorption capacity (mmol/g) and b is the constant related to the free energy of adsorption. K_f is a constant indicative of the relative sorption capacity of the adsorbent (mmol/g) and $1/n$ is the constant indicative of the intensity of the sorption process. If the value of n is greater than 1, it means a strong interaction between the surface of the adsorbent and adsorbate.

A comparison of all fitted isotherms is shown in Figure S6 (available online), and the isotherm parameters and correlation coefficients are summarized in Table 2. It can be found that the adsorption data for Cs^+ and Sr^{2+} fitted more splendidly to the Langmuir model, with higher correlation coefficients compared to the Freundlich model. Meanwhile, for AsO_4^{3-} sorption onto Fe(II)-geopolymer, the Freundlich model was more befitting than the Langmuir model, indicating that the sorption process may be multilayer. In this case, due to $n > 1$ for AsO_4^{3-} sorption onto Fe(II)-geopolymer, it had an increasing tendency for sorption with increasing solid phase concentration. On the other hand, the maximum monolayer sorption capacity values of the adsorbate can be calculated according to the Langmuir model. As for original geopolymer, it had relatively higher maximum adsorption capacity of Cs^+ (0.842 mmol/g) than Sr^{2+} (0.276 mmol/g).

Table 2 | Calculated Langmuir, Freundlich and Dubinin-Radushkevich parameters for the sorption of Cs^+ and Sr^{2+} onto original geopolymer, AsO_4^{3-} onto Fe(II)-geopolymer

Kinetic model	Parameter	Cs^+	Sr^{2+}	AsO_4^{3-}
Langmuir model	Q_m (mmol/g)	0.842	0.276	0.162
	b (L/mmol)	2.003	11.045	3.694
	R_L	0.103	0.050	0.094
	R^2	0.977	0.993	0.902
Freundlich model	n	2.744	5.752	3.289
	K_f (mmol/g)	0.507	0.253	0.121
	R^2	0.965	0.999	0.987
D-R model	β (mol^2/kJ^2)	0.004	0.002	0.003
	q_m (mmol/g)	1.790	0.437	0.329
	E (kJ/mol)	10.937	14.556	12.910
	R^2	0.970	0.993	0.930

In addition, one of the essential characteristics of the Langmuir model can be expressed by a dimensionless constant called equilibrium parameters R_L.

$$R_L = \frac{1}{1 + bC_0} \tag{6}$$

where C_0 is the highest initial metal ion concentration (mmol/L). The value of R_L indicates the type of isotherm to be irreversible ($R_L = 0$), favorable ($0 < R_L < 1$), linear ($R_L = 1$), or unfavorable ($R_L > 1$). As it can be seen in Table 2, all the R_L values for the sorption of Cs^+ and Sr^{2+} onto geopolymer and the sorption of AsO_4^{3-} onto Fe(II)-geopolymer were found to be greater than 0 and less than 1, which indicated the favorable sorption isotherms of these ions.

Furthermore, in order to study the nature of these sorption process, the D-R isotherm was also adopted in the form (Misaelides *et al.* 2018):

$$q_e = q_m e^{-\beta \varepsilon^2} \tag{7}$$

where q_m is the maximum amount of ion that can be sorbed onto unit weight absorbent (mmol/g), and β is the constant related to the sorption energy (mol^2/KJ^2). ε is the Polanyi potential $= RT \ln(1 + 1/C_e)$, where R is the gas constant (8.314 J/mol K), and T is the absolute temperature (K).

In addition, the average free energy of sorption could be the free energy change when the ions are transferred to the surface of adsorbent from the solution. The calculation form is expressed in Equation (8).

$$E = (-2\beta)^{-1/2} \tag{8}$$

where E is the free energy (kJ/mol). Generally, the free energy in the range of 8–16 kJ/mol indicates the cation exchange process, and a value less than 8 kJ/mol suggests physical adsorption, and one greater than 16 kJ/mol implies chemical adsorption (Misaelides *et al.* 2018).

The D-R plots of ln q_e versus ε^2 for these sorption processes are given in Figure S6 and the statistical results are shown in Table 2. It can be seen that the sorption processes of Cs^+ and Sr^{2+} onto original geopolymer have the free energies of 9.561 and 14.556 kJ/mol, respectively. This obviously indicated that the sorption processes for Cs^+ and Sr^{2+} are dominantly ion exchange. However, the energy value for the sorption of AsO_4^{3-} onto Fe(II)-geopolymer was also lower than 16 kJ/mol, suggesting that the mechanism for the removal of AsO_4^{3-} could be not

mainly chemical precipitation, and some other interaction should exist.

Sorption mechanisms

Sorption of Cs^+ and Sr^{2+} onto original geopolymer

Compared to other reported adsorbents (Table S1, available online), the geopolymer and its modified type showed high adsorption abilities for Cs^+ and Sr^{2+}, and AsO_4^{3-}, respectively. Ion exchange with the alkaline ions is considered to be the main reaction in the removal process of Cs^+ and Sr^{2+} by geopolymer, which could be confirmed by the comparisons of released Na^+ with the adsorption amount of Cs^+ and Sr^{2+}, and SEM-EDX mappings, shown in Figures S7 and S8, respectively. The XRD patterns of original geopolymer, Cs-geopolymer and Sr-geopolymer are presented in Figure S9(a). There was neither a new phase nor obvious change occurred between them. FTIR spectra were collected as shown in Figure S10. (Figures S7–S10 are available online.) Compared with the original geopolymer, there was no significant difference between them. As discussed earlier, the weight loss in the range of 160–330 °C is related to bound water molecules connected to the mobile non-framework cations in the cavities of geopolymer. The less weight loss occurred in Cs-geopolymer (1.21%) than that of original geopolymer (1.62%) in the range of 160–330 °C (Figure 3(a)). However, the weight loss of Sr-geopolymer (1.92%) was higher than that of the original geopolymer. This suggests that the amount of water molecules strongly polarized by Sr^{2+} is much higher than those polarized by Na^+ and Cs^+. In this case, hydration numbers of cations should be considered. Specifically, the hydration number (H_n) is the number of those water molecules that undergo strong interaction with ions (Madejová *et al.* 2002). The hydration numbers for Na^+ and Cs^+ are significantly smaller ($H_n = 3.5$ and 2.1, respectively) than for divalent Sr^{2+} ($H_n = 6.4$) (Marcus 1994).

In addition, it is obviously noticed that the original geopolymer has a higher capacity for Cs^+ sorption (0.827 mmol/g) than for Sr^{2+} (0.285 mmol/g). Here, zeolite A, belonging to the framework of cubic space group *Fm3c*, was adopted as a reference. The sorption amount of Sr^{2+} onto zeolite A is generally higher than that of Cs^+ (Vipin *et al.* 2016). Furthermore, Cs^+ is inclined to go through the window to occupy the position of the eight-member ring since it has a large radius size, while Sr^{2+} is more likely to replace with the Na^+ in the six-member ring (Yoshida *et al.* 2013). Therefore, there should be mainly two effects including ring size and charge balance controlling their ion exchange processes onto geopolymer. Theoretically, only an eight-member ring or a large one can accommodate Cs^+ in the structure, and the six-member ring should be the minimum size for Sr^{2+}. On the other hand, there is only an electrical charge on Cs^+, which indicates that Cs^+ can be compensated by only one negative charge produced by the AlO_4 tetrahedron. However, two negative charges would be needed to make a charge balance for Sr^{2+}. Therefore, the arrangement of SiO_4 and AlO_4 tetrahedrons in the geopolymer should be considered. Normally, the ratio of Si/Al in zeolite A is 1 and the arrangement of SiO_4 and AlO_4 tetrahedrons should be alternated (–Si–O–Al–O–Si–O–Al–). If the distance becomes larger, it would be difficult to make a charge balance between Sr^{2+} and the AlO_4 tetrahedron. Theoretically, the Si/Al ratio in the synthesized geopolymer is approximately 1.89. Therefore, there are at least three kinds of arrangements of SiO_4 and AlO_4 in the geopolymer: –Al–O–Si–O–Al–, –Al–Si–O–Si–O–Al– and –Al–Si–O–Si–O–Si–O–Al–. Only the first can provide a proper ion exchange site for Sr^{2+}. It is extremely difficult to quantify their amount in the geopolymer structure because of its amorphous state. But it is confirmable that the arrangement of –Al–O–Si–Al– should be limited. This should be the main reason why the sorption amount of Sr^{2+} is relatively lower than that of Cs^+.

Sorption of arsenate onto Fe(II)-geopolymer

In the present work, the geopolymer was modified and converted into Fe(II) form by a cation exchange process and further applied for AsO_4^{3-} removal. Figure S9(b) presents the XRD patterns of Fe(II) geopolymer before and after sorption. There was no new phase appeared on the XRD pattern of Fe(II) geopolymer after sorption. FTIR spectra of Fe(II) geopolymer before and after sorption are given in Figure 3(b). It can be found that there are two small peaks in the range of 750 to 850 cm^{-1} on the spectrum of Fe(II)-geopolymer after sorption, which could be assigned to the vibrations mode of As-O in arsenate (Sun & Doner 1996). Furthermore, another two peaks occurred at 400–600 cm^{-1}, representing the bond of Fe-O, and this indicated that arsenate removal might be due to the co-precipitation and/or chemisorption of arsenate on iron hydroxide. The spectra of XPS wide scans of Fe(II)-geopolymer before and after sorption are shown in Figure 3(c). Small peaks representing As3d and As3p signals also occurred, which indicated that AsO_4^{3-} had been immobilized on the surface of Fe(II)-geopolymer. It should be convincing that ferrous ion played the key role in the sorption of AsO_4^{3-} onto Fe(II) geopolymer. Figure S11 presents

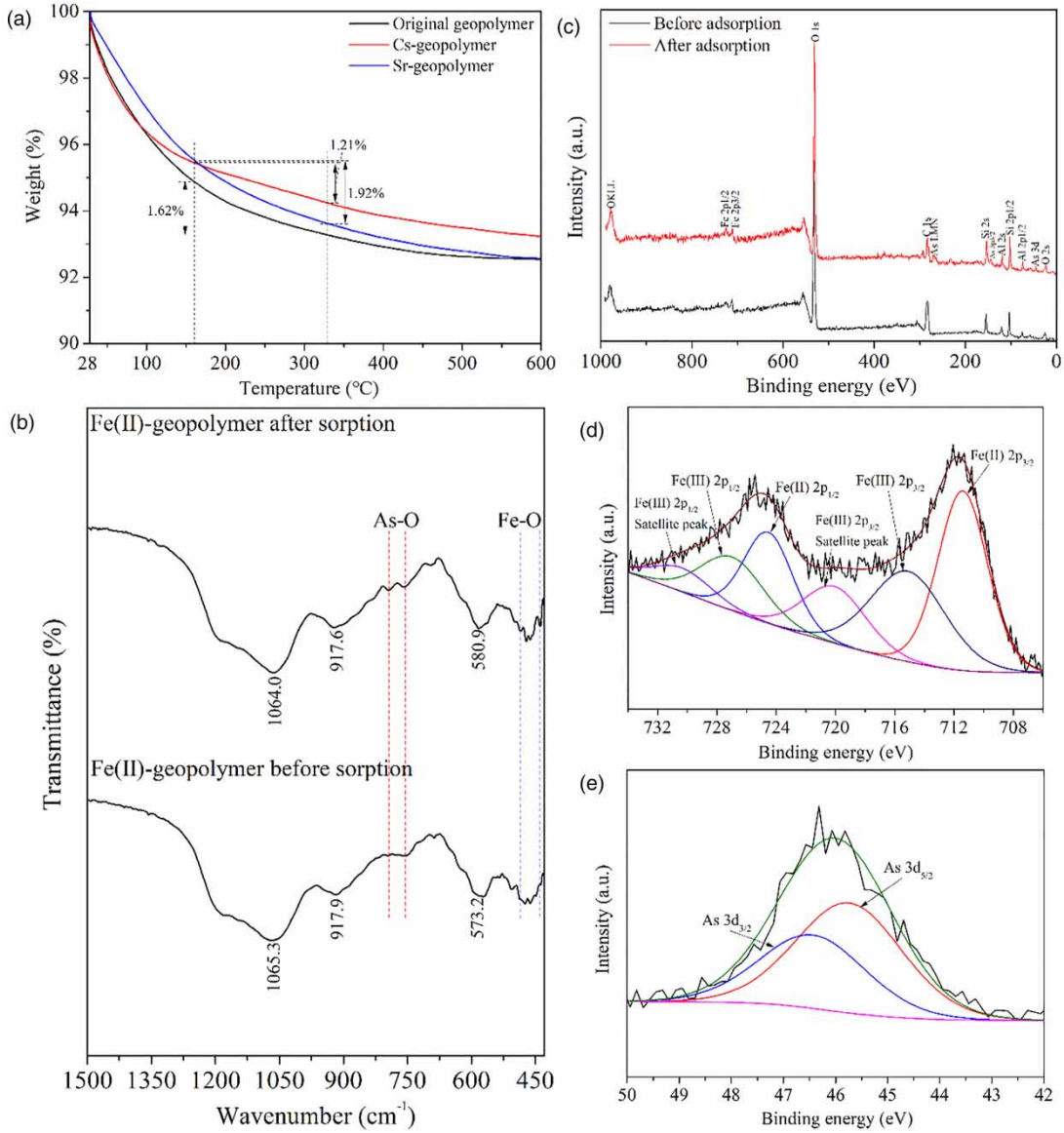

Figure 3 | (a) TG-DTA curves of original geopolymer, Cs-geopolymer and Sr-geopolymer; (b) FTIR spectra of Fe(II)-modified geopolymer before and after sorption of arsenate; (c) XPS wide scan of Fe(II)-geopolymer before and after sorption of arsenate; (d) Fe 2p peak separation of Fe(II)-geopolymer after sorption of arsenate; (e) As 3d peak separation of Fe(II)-geopolymer after sorption of arsenate.

SEM-EDX elemental mapping. The distribution of As showed a good correspondence with the Fe, and this further certified the above deduction. On the other hand, the XPS spectra of Fe 2p peaks for Fe(II) geopolymer before and after sorption are presented in Figure S12. (Figures S11 and S12 are available online.) Compared to the Fe 2p peaks of Fe(II) geopolymer before sorption of AsO_4^{3-}, the two peaks for the adsorbent after sorption exhibited a small shift to higher binding energy. This might imply that Fe(II) might be partially oxidized into Fe(III) during sorption of arsenate. The peak fitting results of Fe and As in Fe(II) geopolymer after sorption are shown in Figure 3(d) and 3(e). The narrow scan for the As 3d spectrum showed characteristic peaks located at 45.7 and 46.4 eV, which were attributed to E_B [As 3d] for AsO_4^{3-} (Muthu Prabhu *et al.* 2018). In addition, the binding energies for Fe^{2+} and Fe^{3+} could be in the range of 709.9–715 and 711.1–719.8 eV (Simsek & Beker 2014). From Figure 3(d), it can be known that a part of Fe(II) has been oxidized into Fe(III), and the molar ratio of Fe(III)/As on the surface of the adsorbent could be calculated using sensitivity factors (Wagner 1983), showing as 0.64. It can be found in Figure S13 (available online) that the concentrations of

dissolved Fe and As adsorption amount showed a reverse trend, which suggested that the removal process of AsO_4^{3-} should be chemical sorption. The chemical formation of $FeAsO_4$ ($K_{sp} \approx 5.8 \times 10^{-21}$ at 25 °C) should be the mainly expected removal mechanism. However, from the calculation results from the D-R isotherm, the free energy (12.91 kJ/mol) was lower than 16 kJ/mol, and the calculated value of Fe/As on the surface of the Fe(II) geopolymer after sorption is obviously lower than the Fe/As ratio in the chemical formula of $FeAsO_4$. This indicates that there might be another sorption mode happening. Specifically, $H_2AsO_4^-$ should be a dominant species in a solution with a pH of 5 (Nicomel *et al.* 2016). After oxidation of Fe^{2+} into Fe^{3+}, some Fe^{3+} might present the formulas of $Fe(OH)_x^{3-x}$ (x = 1 or 2) (Nekhunguni *et al.* 2017). Thus, AsO_4^{3-} sorption might have partially occurred through the formation of inner sphere complexes via ion exchange reaction, which could be predominantly attached by bidentate linkages (Velazquez-Peña *et al.* 2019), as Equation (9) indicates. Thus, precipitation and complexation could be the main mechanisms for AsO_4^{3-} removal using Fe(II)-modified geopolymer.

$$G - Fe(OH)_2^- + 2H_2AsO_4^- \rightarrow G - Fe(OAsO_3H_2)_2^- + 2OH^- \quad (9)$$

CONCLUSIONS

Coal fly ash-based geopolymer and its derivative (Fe(II)-modified geopolymer) were successfully synthesized for removals of Cs^+ and Sr^{2+}, and AsO_4^{3-}, respectively, from aqueous solutions. The results illustrated that the original geopolymer had a much larger surface area (131.4 m^2/g) than coal fly ash (1.1 m^2/g). According to the kinetic fitting results, each sorption process fitted better with the pseudo-second-order model and the overall rate constants appeared to be controlled by chemical sorption. On the other hand, the sorption processes of Cs^+ and Sr^{2+} onto the original geopolymer have better agreement with the Langmuir model. However, the Freundlich model is more befitting for AsO_4^{3-} sorption onto Fe(II) geopolymer. Based on the D-R simulation results, ion exchange is believed to be the main mechanism for sorption of Cs^+ and Sr^{2+} onto the original geopolymer. Specifically, for Cs^+, ring size is the main factor controlling the ion exchange process. However, both ring size and arrangement of SiO_4 and AlO_4 tetrahedrons have the most significant effects on the ion exchange process for Sr^{2+}. This has a close relationship with the molar ratio of Si/Al in the geopolymer structure. On the other hand, for the sorption of AsO_4^{3-} onto Fe(II) geopolymer, chemical formation of $FeAsO_4$ only partially contributes to the removal of AsO_4^{3-} from solution. In addition, AsO_4^{3-} sorption might have occurred through the formation of inner-sphere complexes via ion exchange reaction, which could be predominantly attached by bidentate linkages.

ACKNOWLEDGEMENTS

This research was supported to KS by the JSPS (Japan Society for the Promotion of Science) Kaken Kiban A project (No. JP16H02435) and to TQ by the China Scholarship Council (No. 201706420068).

REFERENCES

Al-Mashqbeh, A., Abuali, S., El-Eswed, B. & Khalili, F. I. 2018 Immobilization of toxic inorganic anions ($Cr_2O_7^{2-}$, MnO_4^- and $Fe(CN)_6^{3-}$ in metakaolin based geopolymers: a preliminary study. *Ceramics International* **44**, 5613–5620.

Benaliouche, F., Hidous, N., Guerza, M., Zouad, Y. & Boucheffa, Y. 2015 Characterization and water adsorption properties of Ag-and Zn-exchanged A zeolites. *Microporous and Mesoporous Materials* **209**, 184–188.

Cho, Y.-K., Yoo, S.-W., Jung, S.-H., Lee, K.-M. & Kwon, S.-J. 2017 Effect of Na_2O content, SiO_2/Na_2O molar ratio, and curing conditions on the compressive strength of FA-based geopolymer. *Construction and Building Materials* **145**, 253–260.

El-Eswed, B. I. 2018 Solidification Versus Adsorption for Immobilization of Pollutants in Geopolymeric Materials: A Review. In: *Solidification*. InTech Open, London, UK, pp. 78–110.

Ho, Y.-S. 2006 Isotherms for the sorption of lead onto peat: comparison of linear and non-linear methods. *Polish Journal of Environmental Studies* **15**, 81–86.

Lin, J. & Wang, L. 2009 Comparison between linear and non-linear forms of pseudo-first-order and pseudo-second-order adsorption kinetic models for the removal of methylene blue by activated carbon. *Frontiers of Environmental Science & Engineering in China* **3**, 320–324.

Lopes, J. H., Nogueira, F. G., Gonçalves, M. & Oliveira, L. C. 2015 Modified zeolite with transition metals Cu and Fe for removal of methylene blue from aqueous medium: mass spectrometry study. *Bulletin of Chemical Reaction Engineering & Catalysis* **10**, 237–248.

Madejová, J., Janek, M., Komadel, P., Herbert, H.-J. & Moog, H. 2002 FTIR analyses of water in MX-80 bentonite compacted from high salinary salt solution systems. *Applied Clay Science* **20**, 255–271.

Marcus, Y. 1994 A simple empirical model describing the thermodynamics of hydration of ions of widely varying charges, sizes, and shapes. *Biophysical Chemistry* **51**, 111–127.

Misaelides, P., Sarri, S., Kantiranis, N., Noli, F., Filippidis, A., de Blochouse, B., Maes, A. & Breynaert, E. 2018 Investigation of chabazitic materials as Cs-137 sorbents from cementitious aqueous solutions. *Microporous and Mesoporous Materials* **266**, 183–188.

Muthu Prabhu, S., Chuaicham, C. & Sasaki, K. 2018 A mechanistic approach for the synthesis of carboxylate-rich carbonaceous biomass-doped lanthanum-oxalate nanocomplex for arsenate adsorption. *ACS Sustainable Chemistry & Engineering* **6**, 6052–6063.

Nekhunguni, P. M., Tavengwa, N. T. & Tutu, H. 2017 Investigation of As(V) removal from acid mine drainage by iron (hydr)oxide modified zeolite. *Journal of Environmental Management* **197**, 550–558.

Nicomel, N., Leus, K., Folens, K., Van Der Voort, P. & Du Laing, G. 2016 Technologies for arsenic removal from water: current status and future perspectives. *International Journal of Environmental Research and Public Health* **13**, 62.

Rożek, P., Król, M. & Mozgawa, W. 2018 Spectroscopic studies of fly ash-based geopolymers. *Spectrochimica Acta Part A: Molecular and Biomolecular Spectroscopy* **198**, 283–289.

Runtti, H., Luukkonen, T., Niskanen, M., Tuomikoski, S., Kangas, T., Tynjälä, P., Tolonen, E.-T., Sarkkinen, M., Kemppainen, K., Rämö, J. & Lassi, U. 2016 Sulphate removal over barium-modified blast-furnace-slag geopolymer. *Journal of Hazardous Materials* **317**, 373–384.

Simsek, E. B. & Beker, U. 2014 Equilibrium arsenic adsorption onto metallic oxides: isotherm models, error analysis and removal mechanism. *Korean Journal of Chemical Engineering* **31**, 2057–2069.

Sun, X. & Doner, H. E. 1996 An investigation of arsenate and arsenite bonding structures on goethite by FTIR. *Soil Science* **161**, 865–872.

Tian, Q., Guo, B., Nakama, S., Zhang, L., Hu, Z. & Sasaki, K. 2019 Reduction of undesirable element leaching from fly ash by adding hydroxylated calcined dolomite. *Waste Management* **86**, 23–35.

Uddin, M. K. 2017 A review on the adsorption of heavy metals by clay minerals, with special focus on the past decade. *Chemical Engineering Journal* **308**, 438–462.

Velazquez-Peña, G. C., Solache-Ríos, M., Olguin, M. & Fall, C. 2019 As (V) sorption by different natural zeolite frameworks modified with Fe, Zr and FeZr. *Microporous and Mesoporous Materials* **273**, 133–141.

Vipin, A. K., Ling, S. & Fugetsu, B. 2016 Removal of Cs^{+} and Sr^{2+} from water using MWCNT reinforced Zeolite-A beads. *Microporous and Mesoporous Materials* **224**, 84–88.

Wagner, C. 1983 Sensitivity factors for XPS analysis of surface atoms. *Journal of Electron Spectroscopy and Related Phenomena* **32**, 99–102.

Yoshida, K., Toyoura, K., Matsunaga, K., Nakahira, A., Kurata, H., Ikuhara, Y. H. & Sasaki, Y. 2013 Atomic sites and stability of Cs^{+} captured within zeolitic nanocavities. *Scientific Reports* **3**, 2457.

First received 21 March 2019; accepted in revised form 8 June 2019. Available online 20 June 2019